Analysis of the Microstructure and Mechanical Properties of Laminated Veneer Lumber

Bing Xue,[a,b] and Yingcheng Hu [a,]*

In this paper, four different nondestructive testing (NDT) methods and static bending tests were done on poplar (*Populus ussuriensis* Kom.) and birch (*Betula platyphylla* Suk.) Laminated Veneer Lumber (LVL). The effects of compression ratio on the modulus of elasticity (*MOE*) and modulus of rupture (*MOR*) of LVL with vertical load and parallel load were investigated. There were four compression ratios: 8.1%, 18.3%, 26.5%, and 33.1%. The microscopic structure of LVL was analyzed with a scanning electron microscope (SEM). Results showed a strong correlation between each dynamic Young's modulus and the static *MOR* of LVL; the *MOE* and *MOR* of LVL changed with the increase of compression ratio. *MOE* and *MOR* were greatly increased when the compression ratio increased from 18.3% to 26.5%, and the microstructure of LVL changed greatly between different compression ratios by birch and poplar species.

Keywords: Laminated veneer lumber (LVL); Compression ratio; Nondestructive testing (NDT); Mechanical properties; Microstructure; Birch; Poplar

Contact information: a: Key Laboratory of Bio-based Material Science and Technology of Ministry of Education of China, College of Material Science and Engineering, Northeast Forestry University, Harbin, 150040, China; b: Heilongjiang Institute of Science and Technology, Harbin, 150027, China;
** Corresponding author: yingchenghu@163.com*

INTRODUCTION

In view of the increasing awareness of society concerning the natural environment, the acceptance of wooden building materials in the form of solid wood and wood-based composites has increased substantially during the past few decades. The main advantages of these materials are availability, renewability, lower processing costs, and simplicity of dismounting and disposal at the end of their service life. Researchers are showing increased interest in the benefits of composite technology for wood-based materials for structural and non-structural usage (Fridley 2002). One of the objectives of composite technology is to produce a product with acceptable performance characteristics using low quality raw materials, combining beneficial aspects of each constituent. New composites are produced with the aim to reduce costs and to improve performance (Schuler and Adair 2003).

Laminated Veneer Lumber (LVL) has been developed as an alternative to solid wood. Veneers obtained from medium- or small-diameter logs are converted into glued parallel laminates or Laminated Veneer Lumber (LVL) which has all the properties of thick wooden planks and it is a useful product for structural purposes. Detailed information on production techniques, technological properties, advantages, and disadvantages of these types of panel products can be found in the literature (Kamala *et al.* 1999; Semra *et al.* 2007).

The field of Nondestructive Testing (NDT) is a very broad, interdisciplinary field that plays a critical role in ensuring that structural components and systems perform their function in a reliable and cost-effective fashion. The utilization of nondestructive testing (NDT) in the evaluation of materials property and performance makes it possible to control the product quality, to monitor equipment operation, to evaluate structure integrity, and to predict residual life of components. NDT has the advantage of not only being prompt, convenient, and time-saving, but also giving great financial benefits (Sinclair 1989; Chen *et al.* 1999). NDT was investigated on poplar lumber and fiber-reinforced plastic (FRP) reinforced fast-growing poplar glulam. Results indicated that the NDT could predict static properties of both wood products. The dynamic Young's modulus values of FRP reinforced the idea that poplar glulam obtained by the dynamic test were generally higher than those by static testing. Reliability of timber structure design based on predicted modulus of rupture (*MOR*) poplar lumber was less than that on measured *MOR* (Cheng and Hu 2011a, b).

The physical and mechanical properties of LVL are significant parameters in the adhibition of LVL, and these properties have been widely studied by researchers working in the field of wood science and technology. But there has been less research aimed at obtaining physical and mechanical properties of LVL through the use of NDT methods or by analysis of the microscopic structure with a scanning electron microscope (SEM) (Dobmann *et al.* 1997; Hu and Afzal 2006).

There are many factors that affect the mechanical properties of LVL, such as the compression ratio, the wood species, veneer drying and aging, size and the density of LVL, and so on (Semra *et al.* 2007; Shukla and Kamdem 2008; Fonselius 1997). The purpose of this study was to analyze the effect of compression ratio and wood species on the mechanical properties of LVL. A further goal was to evaluate the feasibility of using the composite material mechanics analysis method with the NDT testing of LVL. Three analytical methods were used to analyze the mechanical properties of LVL: composite material mechanics, the NDT method, and static testing. In order to analyze the variety of microscopic structures between different compression ratios, the microscopic structure of the LVL was analyzed with SEM.

EXPERIMENTAL

Wood Materials

The rotary-cut veneers were made from poplar (*Populus ussuriensis* Kom.) and birch (*Betula platyphylla* Suk.). The poplar and birch trees were harvested from Inner Mongolia. Round logs obtained from the trees were cut into stocks in rough sizes by taking into consideration final layer dimensions of 600 mm × 500 mm × 3.4 mm (length×width×thickness). A special emphasis was placed on the selection of the wood material. Accordingly, non-deficient, proper, knotless, and normally grown (without zone line, reaction wood, decay, insect, and fungal damages) wood materials were selected, making sure that the growth rings were perpendicular to the surface. The stocks were dried in a drying kiln until a moisture content of 7±1% was reached. These stocks were later used to make 25 mm-thick eight-ply, nine-ply, ten-ply, and eleven-ply LVL in the laboratory.

Preparation of LVL Panels

The LVL panels were bonded with a commercial phenol-formaldehyde (PF) resin. The glue was spread at a rate of 150 g/m^2 onto a single surface of each layer. Glue was spread uniformly on the veneers by manually hand brushing. The glued layers were brought together immediately, one on top of the other, and were kept this way for 30 min before being hot-pressed in a pressing machine for a duration of 40 min under a pressing temperature of 160 ºC and pressure of 1.5 MPa. The target thickness of LVL panels was 25 mm. There were four compression ratios for LVL samples having different numbers of plies: 8.1% for eight-ply samples, 18.3% for nine-ply samples, 26.5% for ten-ply samples, and 33.1% for eleven-ply samples, respectively.

Preparation of Test Samples

Test samples with dimensions of 575 mm × 90 mm × 25 mm and 575 mm × 25 mm × 25 mm were obtained from the LVL panels. The test samples dimension of 575 mm × 90 mm × 25 mm were used in experiments vertical to the glue-line direction load, and the test samples dimension of 575 mm × 25 mm × 25 mm were used in experiments parallel to the glue-line direction load. All test samples were put in an acclimatization chamber, in which the temperature was 20±2 ºC, and the relative humidity was 65±5%, until the weights of the samples remained constant, for the purpose of homogenization of moisture by volume before the experiments. All specimens were tested for the dynamic Young's modulus by NDT testing first, and then MOE and MOR by static testing.

Nondestructive Testing

NDT and static tests of vertical load and parallel load research were conducted to evaluate the mechanical properties of the LVL. The values of the dynamic Young's modulus were obtained by using three different NDT methods, *i.e.* the flexural vibration method (out-plane and in-plane), the longitudinal vibration method, and the longitudinal transmission test (Hu 2004; Hu *et al.* 2005 a, b).

The experiment was first carried out with the flexural vibration method as shown in Figs. 1 and 2. In the test, specimens in the freely vibrating free-free beam test were supported by two planks. The supporting positions of the planks were 0.224 L_s (length of specimen) from both ends. This position corresponds to the nodal points for the fundamental mode of this vibration system. The vibrating frequency was detected by a high-sensitivity microphone connected to a FFT analyzer. The resonant frequencies of the 1st, 2nd, 3rd, and 4th modes were obtained by giving a blow to an edge of the beam and recording the results with the FFT analyzer. The dynamic MOE was obtained from Timoshenko-Goens-Hearmon (TGH) flexural vibration method including the influence of shear and rotatory inertia (Hu 2004).

The experiment was then carried out with the longitudinal vibration method, as shown in Fig. 3. In the test, the specimen was held lightly by the fingers at the center of the specimen while they were tapped by a small hammer at the end of the specimen. The tap tone was detected by a microphone at the other end of the beam. The resonance frequencies of the tap tone were identified by a FFT analyzer. The dynamic MOE was calculated by Eq. 1 (Hu 2004),

$$E_p = \rho\left(\frac{2Lf_n}{n}\right)^2, \; n=1, 2, 3\ldots\ldots \qquad (1)$$

where E_p is dynamic MOE of specimen, L is the length of the specimen, f_n is the resonance frequency, and ρ is the density of the specimen.

The experiment was last carried out with the longitudinal transmission method as shown in Fig. 4. In the test, the sound transmission time propagating through the specimen was measured with a fast Fourier transform (FFT) analyzer. The sound velocity and dynamic MOE were calculated based on Eqs. 2 and 3 (Hu 2004),

$$V = L_S / T \tag{2}$$

$$E_v = \rho V^2 \tag{3}$$

where V is sound velocity, L is length of the specimen, T is transmission time, E_v is dynamic MOE, and ρ is the density of the specimen.

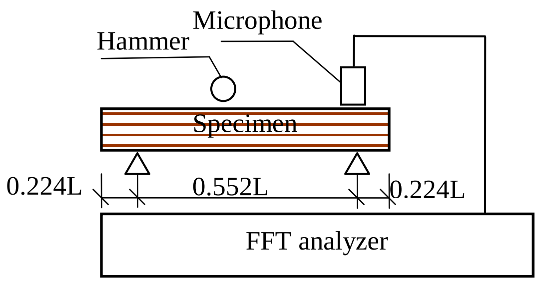

Fig. 1. Out-plane flexural vibration test

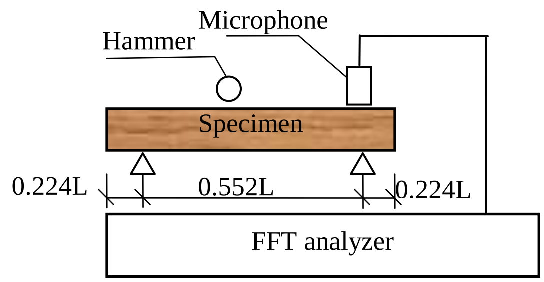

Fig. 2. In-plane flexural vibration test

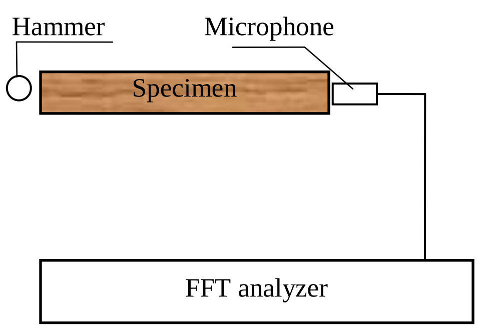

Fig. 3. Longitudinal vibration test

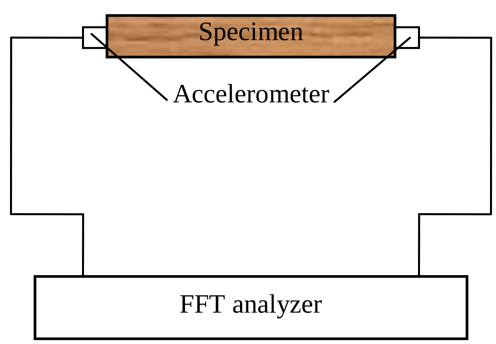

Fig. 4. Longitudinal transmission test

Microscopic Structure Testing

The 1 cm^3 blocks were pre-prepared from LVL specimens. The endgrain was given a cursory polish with a razor blade so that the tangential direction could be located under a dissecting microscope. A second split was made along the tangential surface so that a sample with a polish flat top and bottom was created. Then the samples were observed under electron microscopy after applying a thin layer of gold by sputter-coating. SEM was used to investigate the morphology of samples by using the FEI Model Quanta 200 (FEI Company, USA), and the samples were observed using an applied tension of 12.5 kV. The microscopic structure photos were magnified, the percentage of cell wall was measured with area method and weight method by TDY-5.2 color image computer analysis software packages.

Static Testing

The static bending tests were conducted on the specimens in accordance with the Japanese Agricultural Standard (JAS: SE-11 No. 237: 2003) of Structural Laminated Veneer Lumber. The static *MOR* in bending and modulus of elasticity (*MOE*) in bending was calculated based on Eqs. 4 and 5,

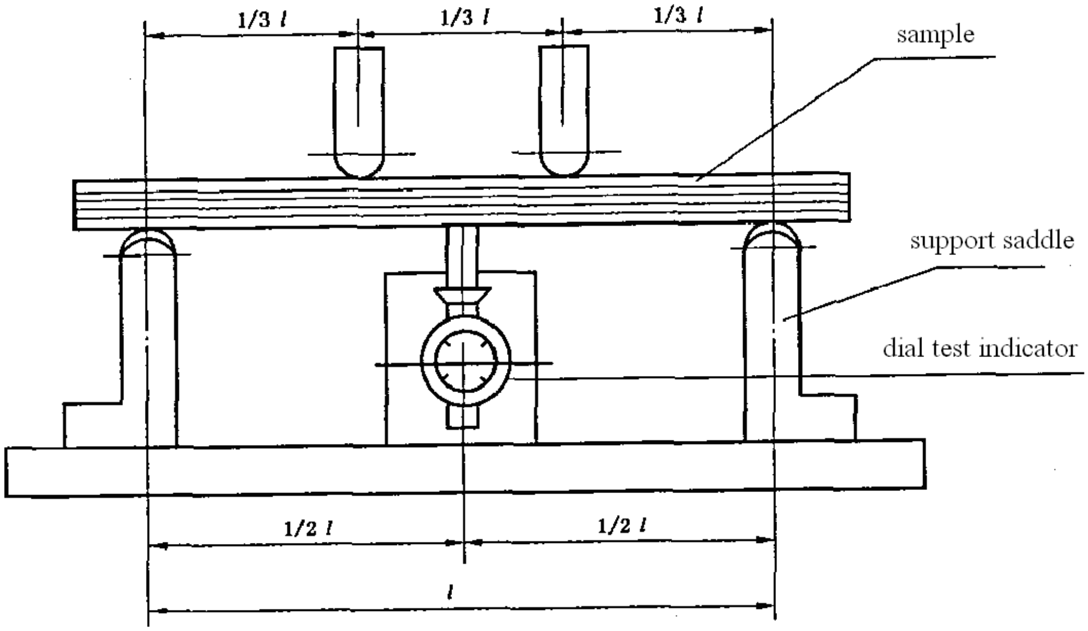

Fig. 5. Vertical load static test

$$MOR = Fl / bh^2 \tag{4}$$

where *MOR* is the modulus of rupture (MPa), *F* is the maximum load (N), *l* is the span in bending between the testing machine grips (mm), *b* is the cross sectional width in the bending test (mm), and *h* is the cross sectional thickness in the bending test (mm).

$$MOE = 23\Delta Fl^3 / 108bh^3\Delta y \tag{5}$$

In Eq. 5, *MOE* is the modulus of elasticity (GPa), ΔF is the increment of load on the regression line with a correlation coefficient of 0.99 or better (N), Δy is the increment of deformation corresponding to F_2 - F_1 (N), and *l, b,* and, *h* are the same as in Eq. 4.

Material Mechanics Analysis

According to previous research (Xue and Hu 2012; Gibson 2011), the following expressions were found by introducing the theoretics of elasticity mechanics,

$$E_C \times V_C = E_L \times V_L \tag{6}$$

where E_c is the static test longitudinal *MOE* of uncompressed clear wood sample, V_c is the volume of uncompressed clear wood sample, E_L is the static test longitudinal *MOE* of LVL sample, and V_L is the volume of LVL sample.

$$\sigma_C \times A_C = \sigma_L \times A_L \tag{7}$$

In Eq. 7, σ_c is the static test longitudinal ultimate pull stress of uncompressed clear wood sample, A_c is the cross-sectional area of uncompressed clear wood sample, σ_L is the static test longitudinal ultimate pull stress of LVL sample, and A_L is the cross-sectional area of LVL sample.

RESULTS AND DISCUSSION

In order to show clearer correlations of every dynamic Young's Modulus of each LVL specimen, the test results of poplar LVL specimen were chosen. The average values of the dynamic Young's modulus and *MOR* are shown in Fig. 6. As shown, the E_v of poplar LVL, dynamic Young's modulus by longitudinal transmission method, was the largest value of all dynamic Young's modulus values. There was little difference between E_1, E_2, and E_p, where the E_1 is dynamic Young's modulus by out-of-plane flexural vibration method, E_2 is dynamic Young's modulus by in-plane flexural vibration method, and E_p is dynamic Young's modulus by longitudinal vibration method, respectively. The trend curve of each NDT test result and *MOR* was very similar.

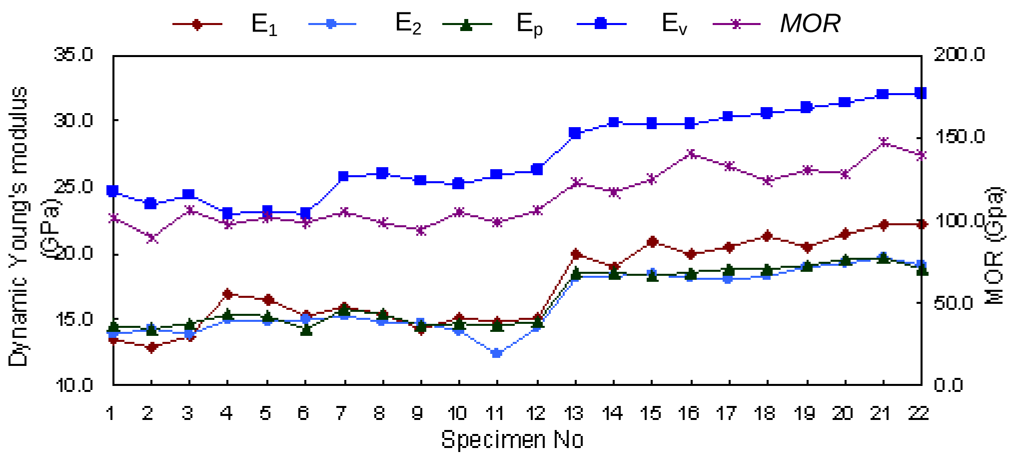

Fig. 6. The values of dynamic Young's modulus of different NDT testing methods and *MOR* of each poplar LVL specimen with vertical load

The regression curves between various dynamic Young's modulus and the *MOR* of all poplar LVL specimens are shown in Fig. 7. From the regression analysis between various dynamic Young's modulus and *MOR*, the linear regression formulas were obtained and shown in Tables 1 and 2. Each correlation coefficient between dynamic Young's modulus and *MOR* was much greater than $R_{20,\ 0.01}$= 0.537. The correlation coefficient of poplar LVL was larger than each of the NDT methods with vertical load, and the correlation coefficient of birch was larger with parallel load. Thus, there was a strong correlation between each dynamic Young's modulus and the static *MOR*; the four different NDT methods can be applied to test the *MOR* of birch and poplar LVL entirely.

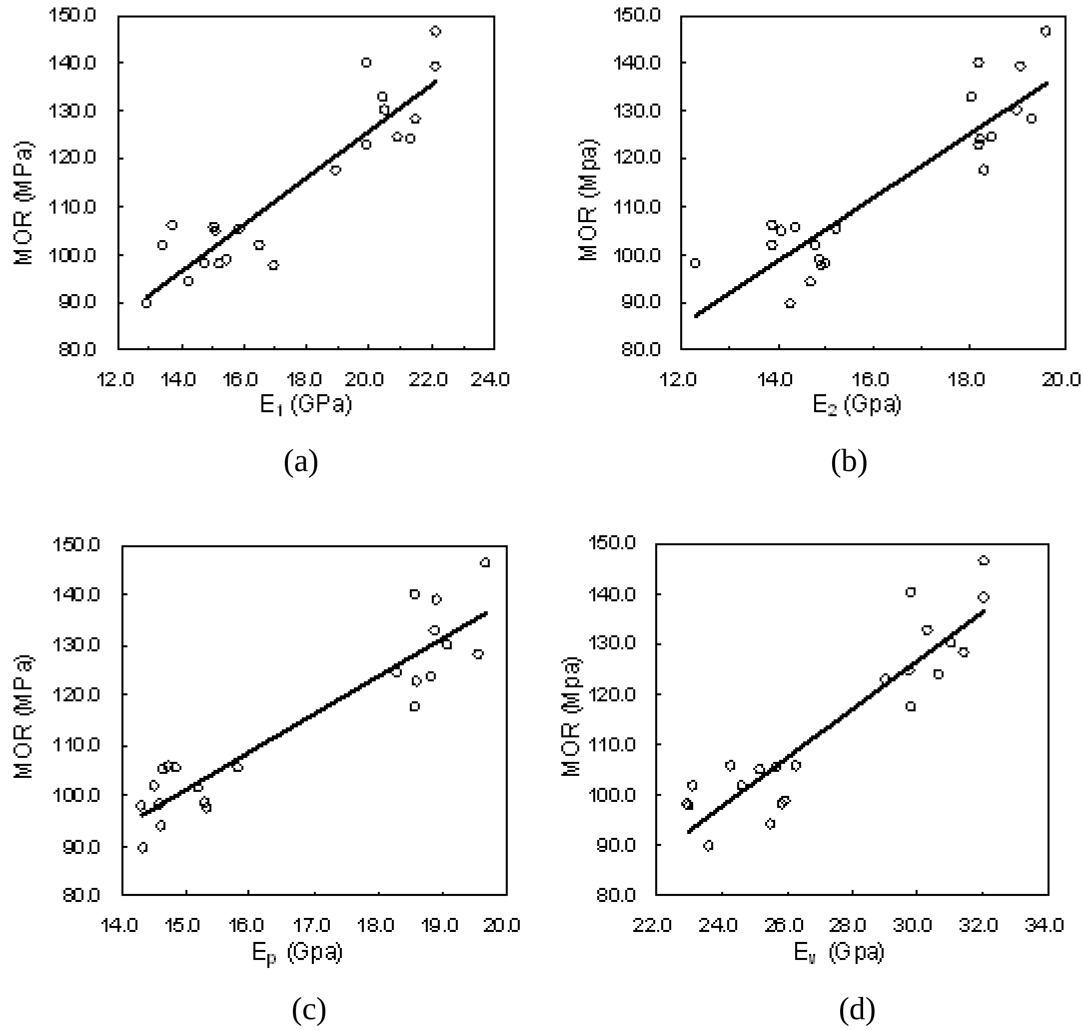

Fig. 7. Regression curve between various dynamic Young's modulus and *MOR* of poplar LVL with vertical load

Table 1. Linear Regression Formula and Correlation Coefficients of Vertical Load

Linear regression formula		Correlation coefficient R	
Birch	Poplar	Birch	Poplar
MOR_1=4.280E_1+43.431	MOR_1=4.903E_1+17.639	R_1 = 0.782	R_1 = 0.914
MOR_2=3.598E_2+57.664	MOR_2=6.701E_2-6.565	R_2 = 0.668	R_2 = 0.899
MOR_p=3.643E_p+54.450	MOR_p=7.483E_p-21.046	R_p = 0.683	R_p = 0.929
MOR_v=2.157E_v+65.167	MOR_v=4.852E_v-28.843	R_v = 0.652	R_v = 0.918

R_1 is correlation coefficient of out-of-plane flexural vibration method, R_2 is correlation coefficient of in-plane flexural vibration method, R_p is correlation coefficient of longitudinal vibration method, and R_v is correlation coefficient of longitudinal transmission method

Table 2. Linear Regression Formula and Correlation Coefficients of Parallel Load

Linear regression formula		Correlation coefficient R	
Birch	Poplar	Birch	Poplar
MOR_1=5.417E_1+3.677	MOR_1=3.211E_1+37.547	R_1 = 0.902	R_1 = 0.856
MOR_2=5.506E_2+1.412	MOR_2=5.668E_2+4.855	R_2 = 0.931	R_2 = 0.941
MOR_p=5.519E_p-1.775	MOR_p=4.869E_p+13.560	R_p = 0.930	R_p = 0.920
MOR_v=4.967E_v+0.367	MOR_v=3.949E_v+14.039	R_v = 0.905	R_v = 0.858

The value of R_1 was greater than that of R_2 for both birch and poplar LVLs in the case of vertical load, whereas the relationship was the reverse in the case of birch and poplar LVLs with parallel load. This was because the direction of striking in the out-of-plane or in-plane flexural vibration method was in accordance with the loading direction of static bending test.

The effects of compression ratio on static testing *MOE* and *MOR* of LVL by vertical load and parallel load are described by Figs. 8 and 9. The *MOE* and *MOR* of birch LVL were larger than poplar LVL (Figs 8 and 9). The mechanical properties of birch LVL was more than poplar LVL. The amplitude of variation of birch LVL *MOE* was larger than poplar LVL; the effects of compression ratio on mechanical properties of birch LVL was less than poplar LVL, and the mechanical properties of birch LVL was relatively stable.

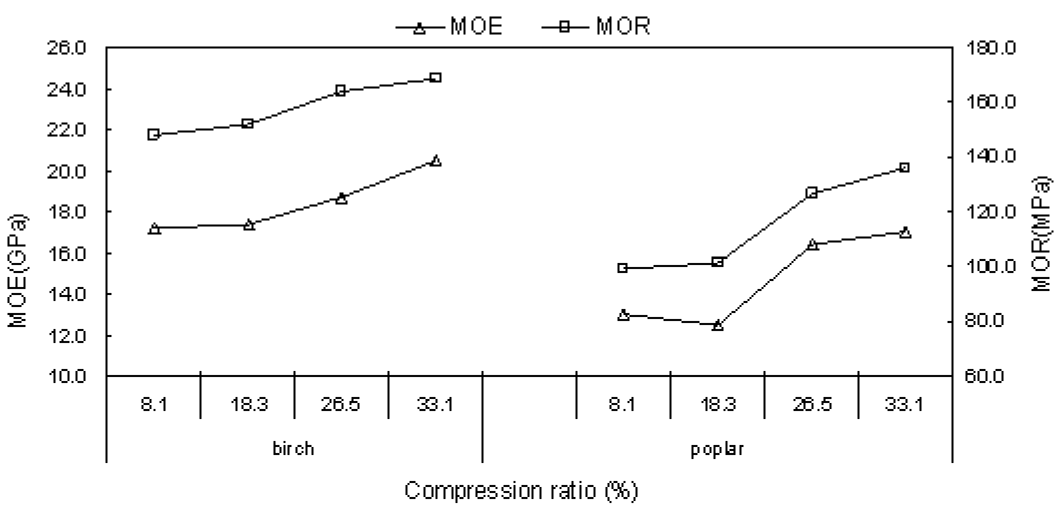

Fig. 8. Effects of compression ratio on static testing *MOE* and *MOR* of LVL with vertical load

The *MOE* and *MOR* of birch LVL increased with an increase of compression ratio with both load methods. Moreover, most *MOE* and *MOR* of poplar LVL increased with an increase of compression ratio with both load methods. While the anomalous data included that among poplar LVL samples, the *MOE* of compression ratio 18.3% was less than 8.1% with two load methods, and the *MOE* and *MOR* of compression ratio 33.1% was less than 26.5% with parallel load. So there were significant effects of the compression ratio on *MOE* or *MOR*. But *MOE* and *MOR* of poplar LVL were not in accordance with this rule entirely, possibly because poplar is a fast-growing wood species and its cell wall structure is unstable. In order to find the reason, the microscopic structure was analyzed in this study.

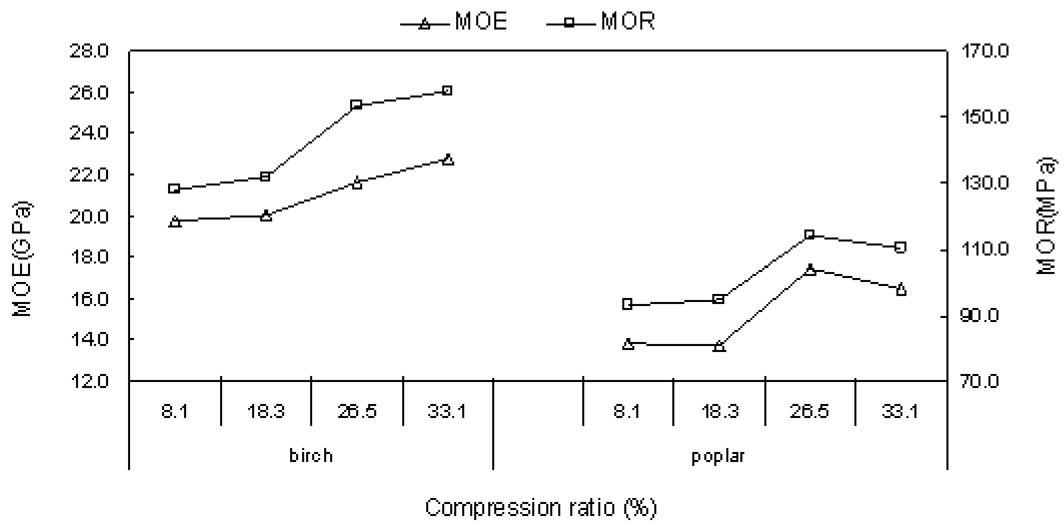

Fig. 9. Effects of compression ratio on static testing *MOE* and *MOR* of LVL with parallel load

The E_C and σ_c theoretical average results and coefficient of variation (COV) of the different compression ratio LVL were obtained by static test results, using Eqs. 6 and 7, and they are presented in Tables 3 and 4.

Table 3. Theoretical Results of Vertical Load

Wood species	Compression ratio (%)	E_C (GPa)	COV of E_C (%)	σ_C (MPa)	COV of σ_C (%)
Birch	8.1	15.361	1.690	132.123	4.901
	18.3	14.129	0.872	123.292	4.987
	26.5	14.040	1.654	123.213	5.883
	33.1	14.182	3.101	117.002	6.389
Poplar	8.1	11.583	12.744	88.354	5.001
	18.3	9.917	4.654	80.454	4.492
	26.5	11.712	3.857	90.643	5.881
	33.1	11.252	6.007	89.851	5.089

Table 4. Test and Theoretical Results of Parallel Load

Wood species	Compression ratio (%)	E_C (GPa)	COV of E_C (%)	σ_C (MPa)	COV of σ_C (%)
Birch	8.1	13.409	2.762	119.623	5.390
	18.3	13.493	1.910	108.766	2.095
	26.5	14.679	8.240	114.247	7.645
	33.1	15.512	5.301	107.478	2.699
Poplar	8.1	9.377	1.200	86.565	5.825
	18.3	9.331	4.330	78.891	3.356
	26.5	11.919	4.056	85.530	2.574
	33.1	11.291	7.389	75.343	6.062

According to Tables 3 and 4, the average of birch and poplar vertical load E_C was 14.418 and 11.116 GPa, respectively, and the parallel load E_C was 14.273 and 10.479 Gpa, respectively. The average of birch and poplar vertical load σ_C was 123.901 and

87.326 MPa, respectively, and the parallel load σ_C was 112.529 and 81.582 MPa, respectively. These data are similar to the congeneric data in some interrelated references (Bodig and Jayne 1982; Liu 2004; Long 2005). Most COVs of E_C and σ_C were under 10%, and the results were very steady. Thus, Eqs. 6 and 7 were judged to be workable, on a rudimentary level, but the half E_C and σ_C of compression ratio 33.1% was less than 26.5% with two load methods.

As mentioned above, the *MOE* and *MOR* of the larger compression ratio LVL was less than that of the smaller compression ratio LVL. In order to explain this phenomenon, the microscopic structure of LVL was observed with SEM and is described by Figs. 10 and 11.

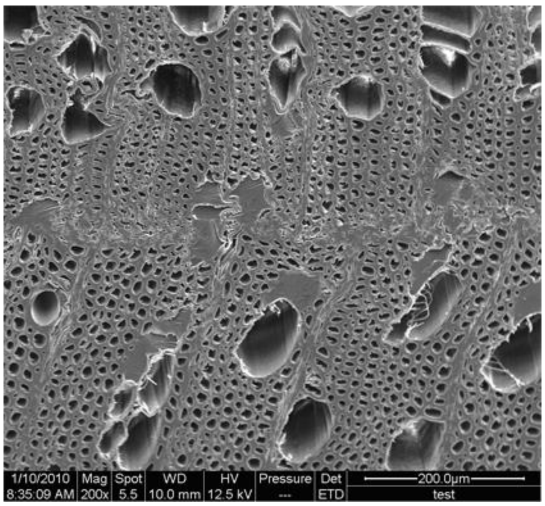

eight-ply sample

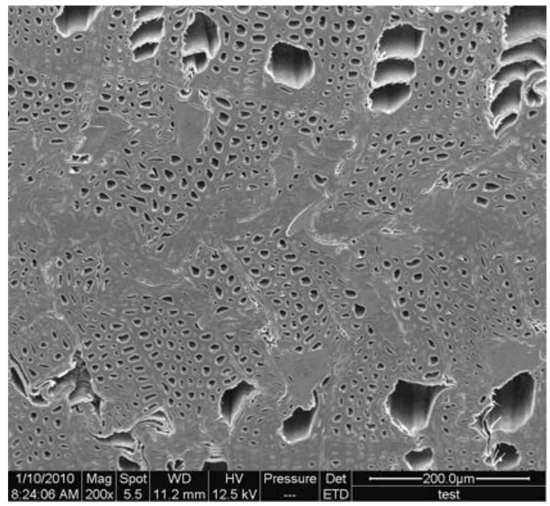

nine-ply sample

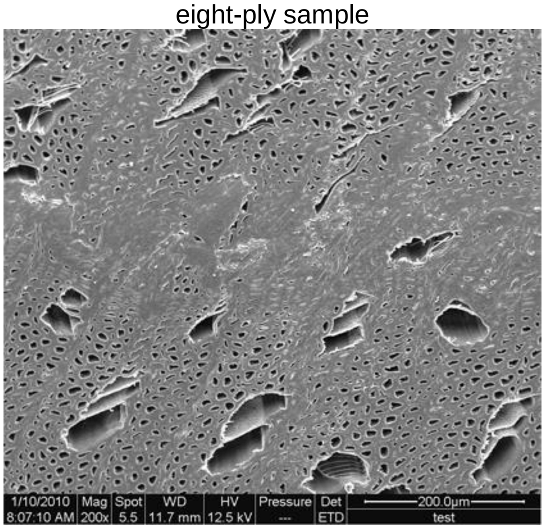

ten-ply sample

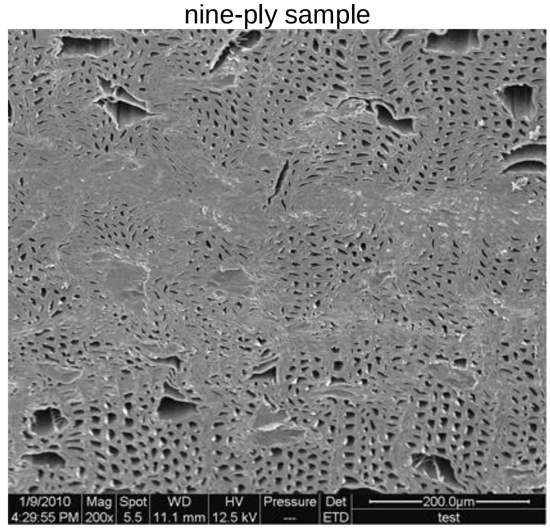

eleven-ply sample

Fig. 10. The microscopic structure of birch LVL

According to Fig. 10, the dimensions of vessels decreased as the compression ratio increased, and the lumina near the glue line were compressed slightly. There was no compression failure in the birch sample subject to different compression ratios, so the *MOE* and *MOR* increased with the increase of compression ratio.

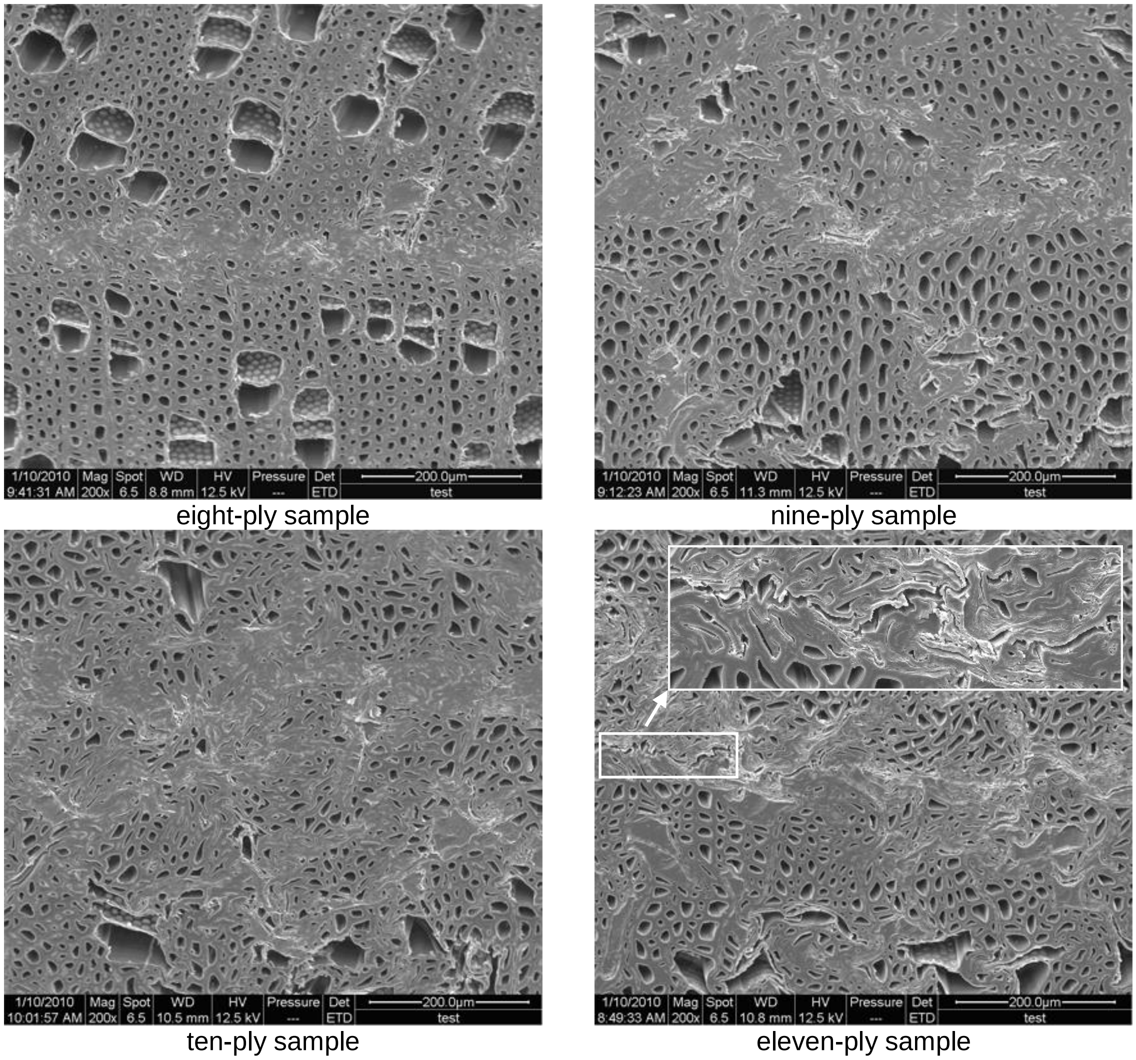

Fig. 11. The microscopic structure of poplar LVL

Figure 11 shows more changes of vessels than Fig. 10, and there were some horizontal cracks and some small compression failure in the eleven-ply sample. Therefore, the *MOE* and *MOR* was less in the eleven-ply sample compared to the ten-ply sample with parallel load.

According to the SEM photos, the cell wall tissue textures of eight-ply samples were intact after being hot pressed, but some cells were compressed in part. The vessel sections were compressed in the nine-ply, ten-ply, and eleven-ply samples. Moreover, there was distinct compression and some small compression failure in eleven-ply samples of poplar. Thus, the *MOE* of eleven-ply was less than that of the ten-ply sample with vertical load. The pressure on veneer increased as the compression ratio increased, and the density of cell tissue structure increased accordingly. But the tissue experienced compression failure and generated plastic deformation when the compression ratio exceeded a certain limit, resulting in a decline of the mechanical properties of LVL. Because poplar material was softer than birch, the compression ratio limit of poplar was low.

In order to verify the analysis of the mechanical test results, the percentage of cell wall was analyzed, as described by Fig. 12. The percentages of cell wall of eleven-ply were less than ten-ply all, and nine-ply was less than eight-ply of poplar LVL. This explained why some *MOE* and *MOR* of eleven-ply poplar LVL were less than ten-ply, and the *MOE* of nine-ply was less than eight-ply poplar LVL. The comparison was consistent between mechanical properties and SEM results. The compression ratio should be under 26.5% when processing poplar LVL, because there were small failure cells in the earlywood of eleven-ply samples. The change of percentage of cells was not fully consistent with mechanical properties of LVL, because the sampling size of SEM photos was very small, and the percentage of cells of whole LVL could not be displayed fully.

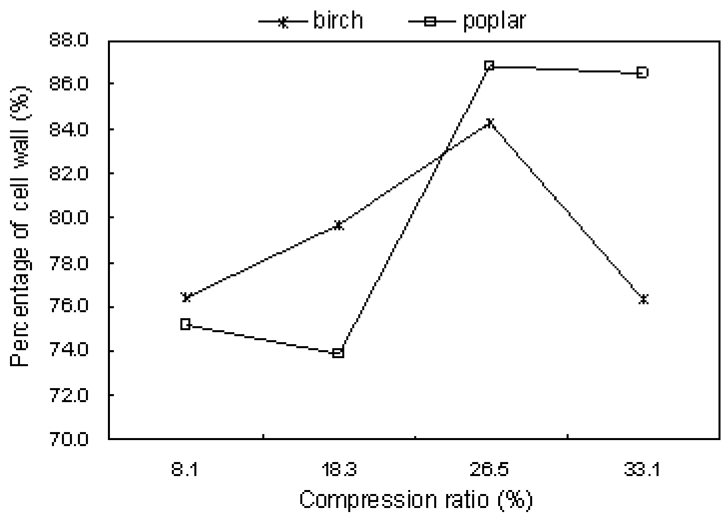

Fig. 12. Effects of compression ratio on the percentage of cell wall of LVL

There were some cracks and some small compression failure in the eleven-ply sample of poplar LVL, so the compression ratio should be under 26.5% when processing poplar LVL, and the Eqs. 6 and 7 were not calculated for eleven-ply sample of poplar LVL. So these will not be included in the following exposition.

The thickness of veneers was 3.4 mm, which is much less than the dimension of length and breadth. Thus, Poisson’s ratio of veneers can be ignored, and the veneers exhibit deformation with respect to thickness only after hot-pressing. So the compression ratio were introduced to Eqs. 6 and 7, and Eqs. 8 and 9 could be obtained,

$$E_L = \frac{E_C}{1-\varphi_E C_R} \tag{8}$$

$$\sigma_L = \frac{\sigma_C}{1-\varphi_R C_R} \tag{9}$$

where C_R is the actual compression ratio of LVL, φ_E and φ_R are correction factors of compression ratio, and other variables are the same as Eqs.6 and 7.

The status was analyzed when φ_E and φ_R were equal to 1.0 firstly. When both E_C and σ_c of birch and poplar with vertical and parallel load were taken into Eqs. 8 and 9, the theoretical result of E_L and σ_L could be obtained. The average deviation rates between the test result and theoretical result of the different compression ratios LVL using Eqs. 8 and 9 could be obtained. And the majority average deviation rates between the test result and theoretics result of E_L were positive. Thus, Eq. 8 was relatively reliable, noting that the test result was greater than the theoretical result. But there were two negative value deviation rates, -9.835% and -7.561% in the results. Those were less than -5% and unreliable. And about half of the average deviation rates between the test result and theoretics result of σ_L were postitive, so Eq. 9 was judged to be unreliable. In addition there were errors on the thickness of the veneer. So the correction factors φ_E and φ_R should be under 1.0. The average deviation rates between the test result and theoretics result of E_L and σ_L are presented in Tables 5 and 6 when φ_E and φ_R equal to 0.95.

Table 5. Average Deviation Rates between the Test Result and Theoretics Result of E_L (%)

Compression ratio (%)	Vertical load		Parallel load	
	Birch	Poplar	Birch	Poplar
8.1	10.786	9.252	10.201	5.571
18.3	3.026	-3.911	2.710	-4.600
26.5	2.379	14.700	2.985	11.445
33.1	3.295	-	0.013	-

Table 6. Average Deviation Rates between the Test Result and Theoretics Result of σ_L (%)

Compression ratio (%)	Vertical load		Parallel load	
	Birch	Poplar	Birch	Poplar
8.1	10.930	7.045	6.440	0.974
18.3	4.562	-0.050	0.294	2.001
26.5	4.502	13.898	7.311	9.537
33.1	-0.677	-	2.432	-

According to Tables 5 and 6, the majority of the average deviation rates between the test result and theoretics result of E_L and σ_L were plus, and the smallest result of deviation rates of E_L and σ_L were -4.600% and -3.071%, respectively, and those were greater than -5%. So Eqs. 8 and 9 were reliable when φ_E and φ_R were equal to 0.95. Both equations can be applied to the *MOE* and *MOR* prediction of birch and poplar LVLs.

CONCLUSIONS

1. There was a strong correlation between each dynamic Young's modulus and the static *MOR* of birch and poplar LVLs. The four different NDT methods can be applied to the *MOR* prediction of birch and poplar LVLs entirely.
2. The *MOE* and *MOR* of birch LVL increased with increasing compression ratio with both load methods, but the poplar LVL was not in accordance with this rule entirely.

3. When φ_E and φ_R equaled 0.95, Eqs. 6 and 7 were reliable and can be used for mechanical properties prediction of various compression ratio birch and poplar LVL.
4. The microscopic structure of LVL was observed with a scanning electron microscope. Earlywood was the main location where compressional change was manifested. The compression ratio should be under 26.5% when processing poplar LVL.

ACKNOWLEDGMENTS

This project was supported by the Fundamental Research Funds for the Central Universities (DL12EB03), the National Natural Science Foundation of China (31170516, 31010103905), and the Scientific Research Fund of Heilongjiang Provincial Education Department (NO: 12511488).

REFERENCES CITED

Bodig, J., and Jayne, B. A. (1982). *Mechanics of Wood and Wood Composites*, Van Nostrand and Reinhold, New York.

Chen, J., Shi, Y., and Shi, S. (1999). "Noise analysis of digital ultrasonic nondestructive evaluation system," *International Journal of Pressure Vessels and Piping* 76(9), 619-630.

Cheng, F. C., and Hu, Y. C. (2011a). "Reliability analysis of timber structure design of poplar lumber with nondestructive testing methods," *BioResources* 6(3), 3188-3198.

Cheng, F. C., and Hu, Y. C. (2011b). "Nondestructive test and prediction of *MOE* of FRP reinforced fast-growing poplar glulam," *Composites Science and Technology* 71(8), 1163-1170.

Dobmann, G., Meyendorf, N., and Schneider, E. (1997). "Nondestructive characterization of materials: a growing demand for describing damage and service-life-relevant aging process in plant components," *Nuclear Engineering and Design* 171(1-3), 95-112.

Fonselius, M. (1997). **"**Effect of size on the bending strength of laminated veneer lumber," *Wood Science and Technology* 31(6), 399-413.

Fridley, K. (2002). "Wood and wood-based materials: Current status and future of a structural material," *J. Mater. Civ. Eng.* 14(2), 91-96.

Gibson, R. F. (2011). *Principles of Composite Material Mechanics*, CRC Press, Boca Raton.

Hu, C. S., and Afzal, M. T. (2006). "A statistical algorithm for comparing mode shapes of vibration testing before and after damage in timbers," *J. Wood Sci.* 52(4), 348-352.

Hu, Y. C. (2004). *Dynamic Properties and Nondestructive Test of Wood-based Composites*, Northeast Forestry University Press, Harbin. (in Chinese).

Hu, Y. C., Nakao, T., Nakai, T., Gu, J. Y., and Wang, F. H. (2005a). "Dynamic properties of three types of wood-based composites," *J. Wood Sci.* 51(1), 7-12.

Hu, Y. C., Wang, F. H., Gu, J. Y., Liu, Y. X., and Nakao, T. (2005b). "Nondestructive test and prediction of modulus of elasticity of veneer-overlaid particleboard composite," *Wood Sci. Technol.* 39(6), 439-447.

Kamala, B. S., Kumar, P., Rao, R.V., and Sharma, S. N. (1999). "Performance test of laminated veneer lumber (LVL) from rubber wood for different physical and

mechanical properties," *Holz Roh-und Werkstoff* 57(2), 114-116.
Liu, Y. X. (2004). *Woodiness Resource Materials Science*, China Forestry publishers, Beijing (in Chinese).
Long, W. G. (2005). *Wood Structure Design Handbook*, China Architecture & Building Press, Beijing (in Chinese).
Semra, Ç., Gürsel, Ç., and Ismail, A. (2007). "Effects of logs steaming, veneer drying and aging on the mechanical properties of laminated veneer lumber (LVL)," *Building and Environment* 42(1), 93-98.
Schuler, A., and Adair, C. (2003). "Engineered and other wood products–An opportunity to 'grow the pie'," In: *37th International Wood Composite Materials Symposium*, 43-53.
Shukla, S. R., and Kamdem, D. P. (2008). "Properties of laminated veneer lumber (LVL) made with low density hardwood species: Effect of the pressure duration," *Holz Roh-und Werkstoff* 66(2), 119-127.
Sinclair, A. A. (1989). "Analysis of ultrasonic frequency response for flaw detection: A technique review," *Materials Evaluation* 47(3), 314-316.
Xue, B., and Hu, Y. C. (2012). "Mechanical properties analysis and reliability assessment of laminated veneer lumber (LVL) having different patterns of assembly," *BioResources* 7(2), 1617-1632.

Article submitted: December 29, 2012; Peer review completed: March 19, 2013; Revised version received and accepted: April 10, 2013; Published: April 11, 2013.